

Improved luminescence properties by self-assembly of lanthanide compounds with 1-D chain structure for sensing of CH₃COOH and toxic HS⁻ anions

Yuan-Yi Xu,^a Peng Chen,^a Ting Gao,^{*a} Hong-Feng Li^a and Peng-Fei Yan^a

^a Key Laboratory of Functional Inorganic Material Chemistry (MOE), School of Chemistry and Materials Science, Heilongjiang University, No. 74, Xuefu Road, Nangang District, Harbin 150080, P.R. China. E-mail: gaotingmail@sina.cn.

Synthesis of complexes 1, 3, 4 and doped compounds

[Sm₂L(TTA)₄(OAc)₂]_n (1). Yield: 0.169g (45.7%). Elemental analysis (%) calcd for C₂₈H₂₂F₆GdNO₇S₂ (812.95): C, 41.33; H, 2.71; N, 1.72. found: C, 41.30; H, 2.70; N, 1.73; IR (KBr, cm⁻¹): 3058 (w), 2946 (s), 2733 (w), 2690(w), 1692 (vs), 1684 (vs), 1532 (s), 1431 (vs), 1302 (s), 1245 (vs), 1156 (m), 1104 (m), 961 (vs), 884 (w), 722 (m), 643 (w), 589 (m). UV-vis [MeOH, λ]: 211, 254, 348 nm.

[Gd₂L(TTA)₄(OAc)₂]_n (3). Yield: 0.176g (47.2%). Elemental analysis (%) calcd for C₂₈H₂₂F₆GdNO₇S₂ (819.84): C, 40.98; H, 2.68; N, 1.71. found: C, 41.00; H, 2.67; N, 1.70; IR (KBr, cm⁻¹): 3062 (w), 2945 (s), 2734 (w), 2688(w), 1689 (vs), 1684 (vs), 1534 (s), 1429 (vs), 1299 (s), 1240 (vs), 1154 (m), 1103 (m), 962 (vs), 885 (w), 721 (m), 642 (w), 590 (m). UV-vis [MeOH, λ]: 211, 254, 348 nm.

[Yb₂L(TTA)₄(OAc)₂]_n (4). Yield: 0.181g (48.2%). Elemental analysis (%) calcd for C₂₈H₂₂F₆GdNO₇S₂ (835.63): C, 40.21; H, 2.63; N, 1.68. found: C, 41.19; H, 2.63; N, 1.67; IR (KBr, cm⁻¹): 3058 (w), 2941 (s), 2728 (w), 2692(w), 1687 (vs), 1681 (vs), 1538 (s), 1432 (vs), 1296 (s), 1242 (vs), 1151 (m), 1101 (m), 963 (vs), 882 (w), 720 (m), 644 (w), 590 (m). UV-vis [MeOH, λ]: 211, 254, 348 nm.

[(Sm_xGd_{1-x})₂L(TTA)₄(OAc)₂]_n IR (KBr, cm⁻¹): 3060 (w), 2950 (s), 2740 (w), 2691(w), 1692 (vs), 1681 (vs), 1533 (s), 1435 (vs), 1301 (s), 1242 (vs), 1153 (m), 1098 (m), 962 (vs), 880 (w), 719 (m), 645 (w), 583 (m). UV-vis [MeOH, λ]: 211, 254, 348 nm.

$[(\text{Eu}_x\text{Gd}_{1-x})_2\text{L}(\text{TTA})_4(\text{OAc})_2]_n$ IR (KBr, cm^{-1}): 3055 (w), 2945 (s), 2736 (w), 2688(w), 1693 (vs), 1684 (vs), 1536 (s), 1430 (vs), 1303 (s), 1245 (vs), 1156 (m), 1105 (m), 963 (vs), 881 (w), 720 (m), 644 (w), 585 (m). UV-vis [MeOH, λ]: 211, 254, 348 nm.

$[(\text{Yb}_x\text{Gd}_{1-x})_2\text{L}(\text{TTA})_4(\text{OAc})_2]_n$ IR (KBr, cm^{-1}): 3057 (w), 2946 (s), 2733 (w), 2687(w), 1691 (vs), 1682 (vs), 1538 (s), 1431 (vs), 1297 (s), 1246 (vs), 1154 (m), 1104 (m), 961(vs), 882 (w), 722 (m), 641 (w), 582 (m). UV-vis [MeOH, λ]: 211, 254, 348 nm.

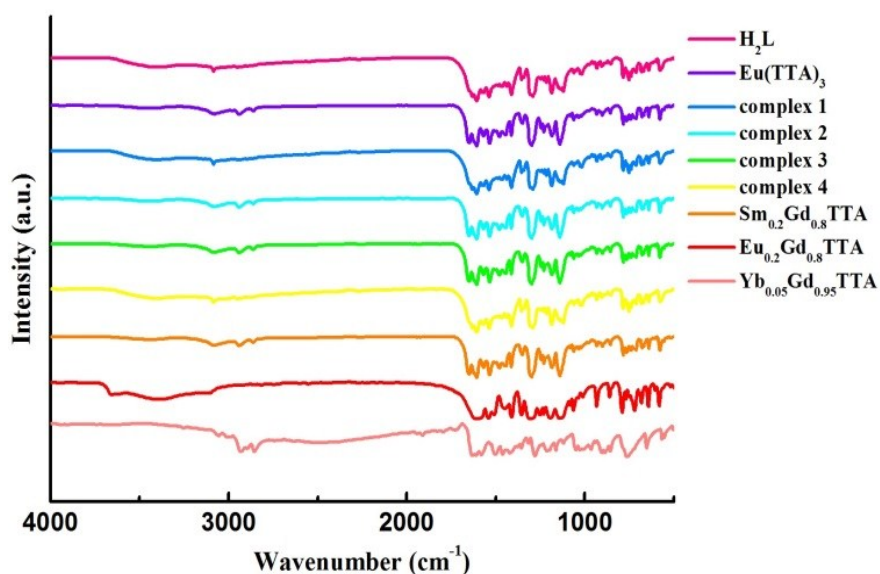


Fig.S1 IR spectra of H_2L , $\text{Eu}(\text{TTA})_3$, complexes 1-4 and $\text{Ln}_x\text{Gd}_{1-x}\text{TTA}$.

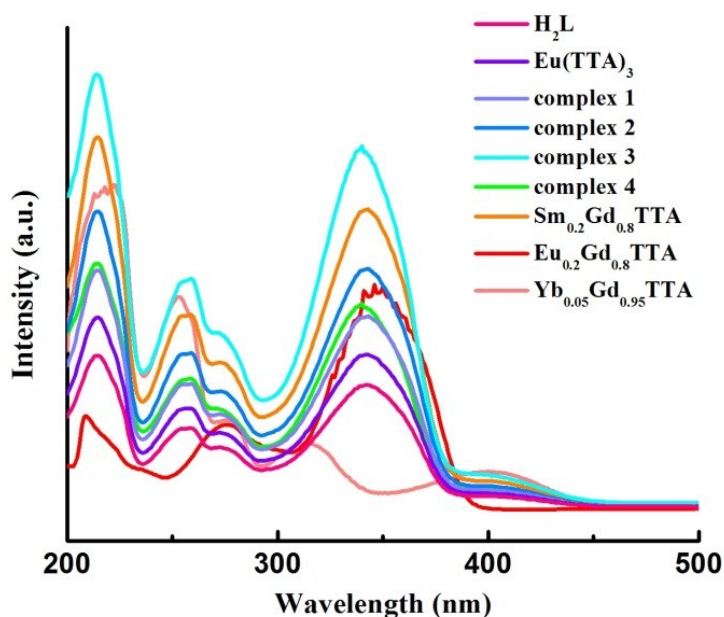


Fig.S2 UV-vis absorption spectra of H_2L , $\text{Eu}(\text{TTA})_3$, complexes 1-4 and $\text{Ln}_x\text{Gd}_{1-x}\text{TTA}$.

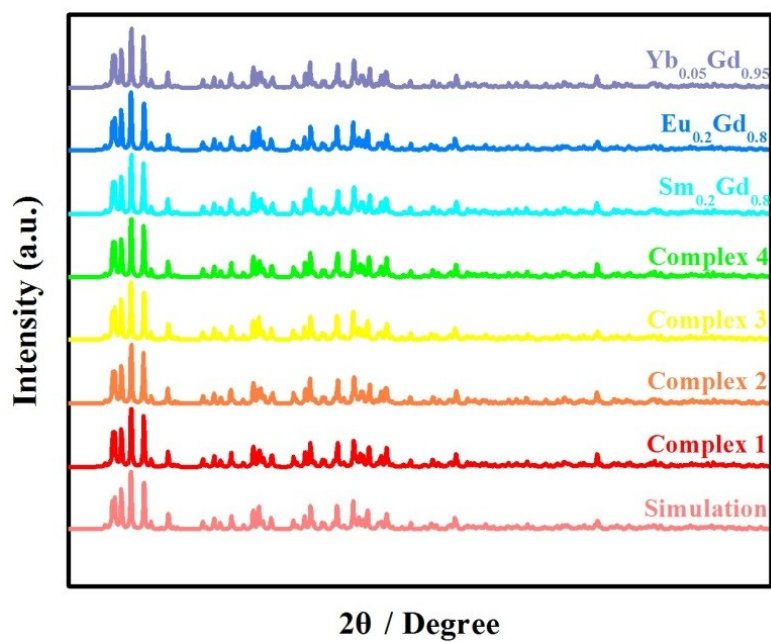


Fig.S3 PXR D patterns for simulation, complexes 1-4 and $\text{Ln}_x\text{Gd}_{1-x}\text{TTA}$.

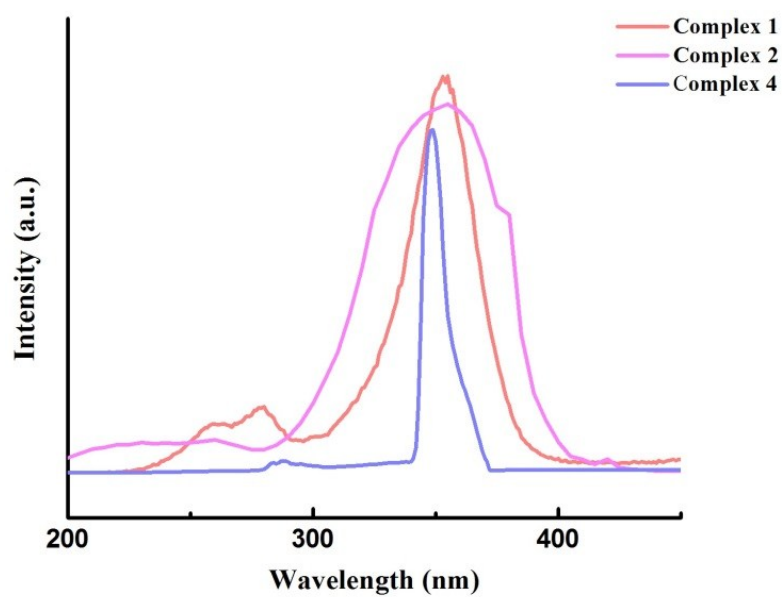


Fig.S4 The excitation spectra of complexes 1, 2 and 4 in the solid state.

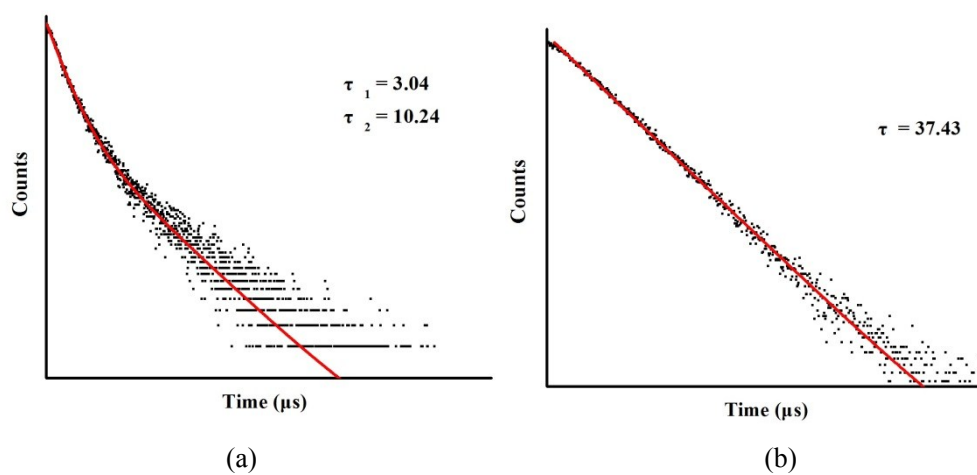


Fig.S5 (a) Luminescence decay profile for complex **1** in the solid state; (b) Luminescence decay profile for doped complex **Sm_{0.2}Gd_{0.8}TTA** in the solid state.

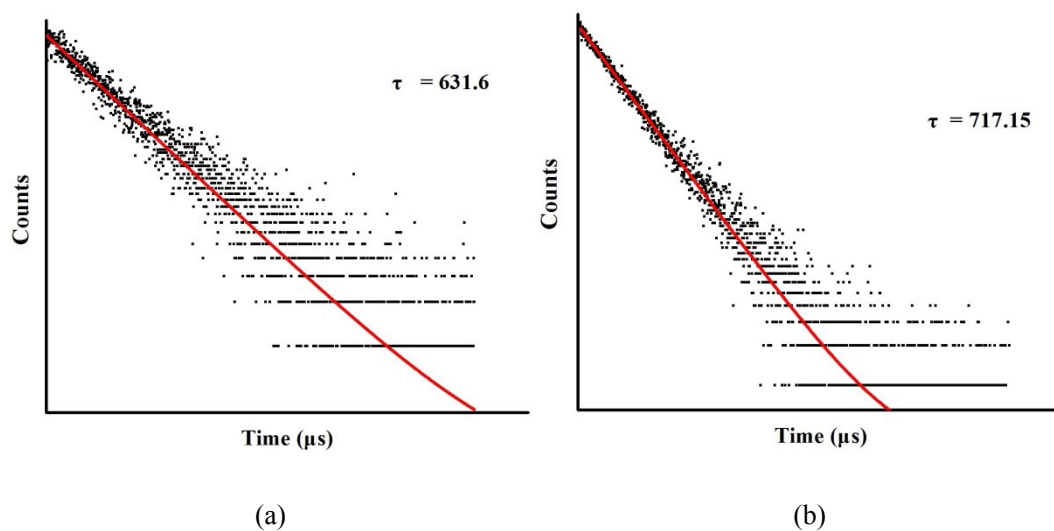


Fig.S6 (a) Luminescence decay profile for complex **2** in the solid state; (b) Luminescence decay profile for doped complex **Eu_{0.2}Gd_{0.8}TTA** in the solid state.

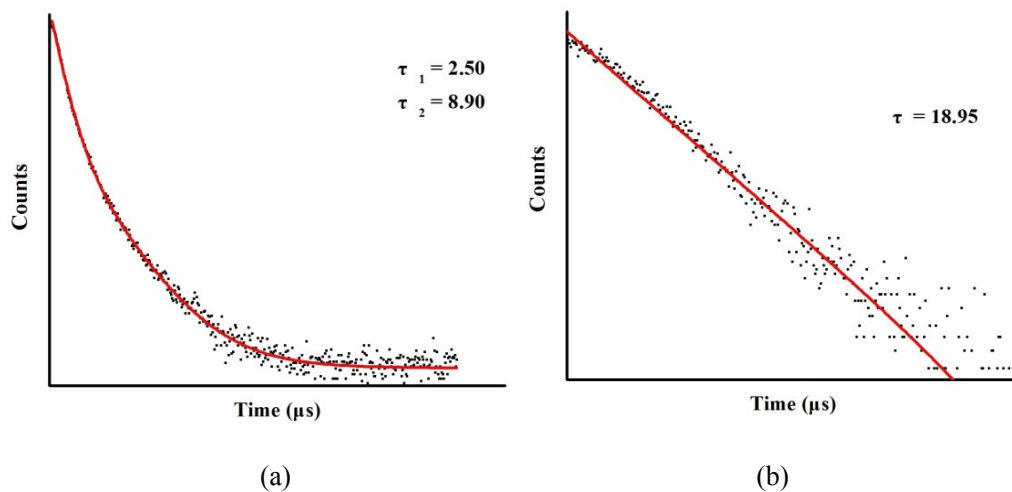


Fig.S7 (a) Luminescence decay profile for complex **4** in the solid state; (b) Luminescence decay profile for doped complex $\text{Yb}_{0.05}\text{Gd}_{0.95}\text{TTA}$ in the solid state.

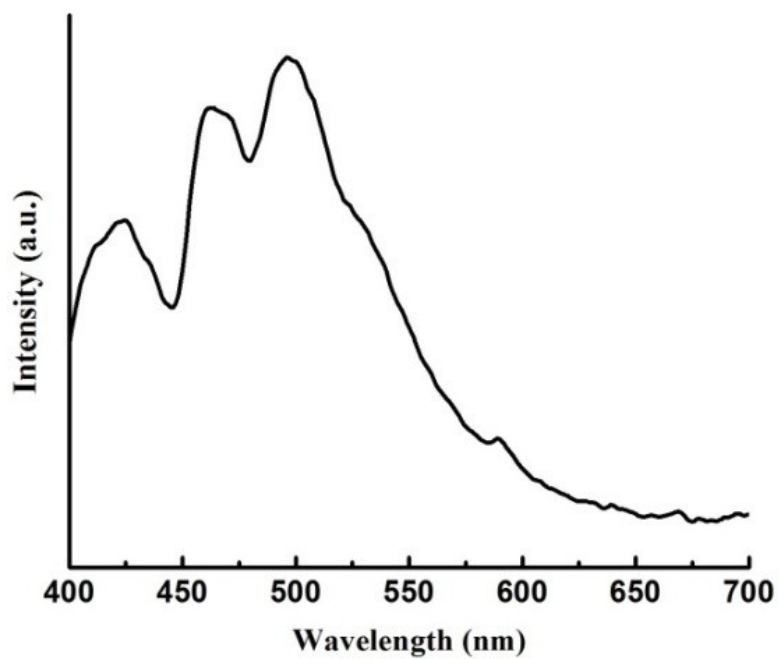
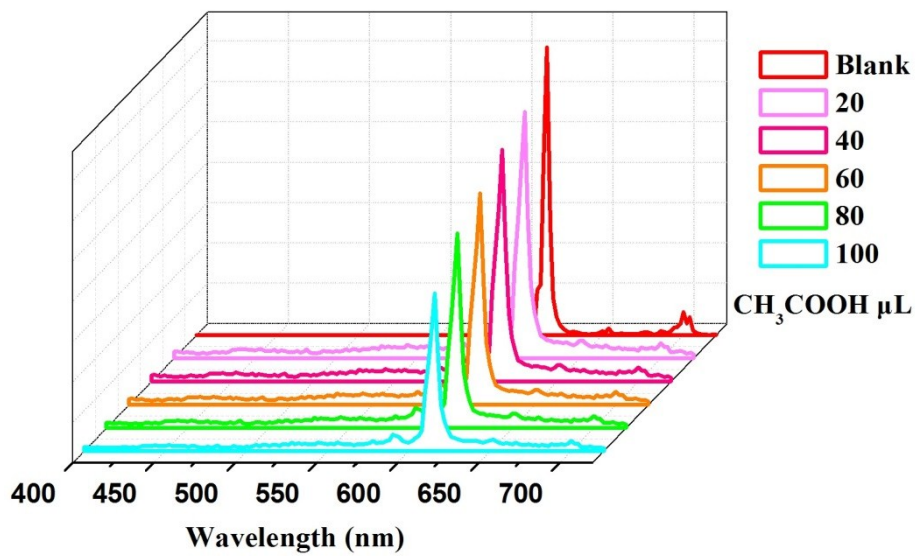
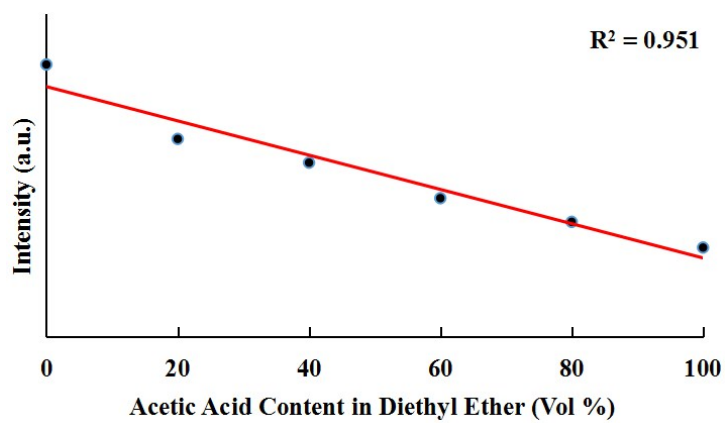


Fig.S8 Phosphorescence spectrum of $\text{Gd}_2\text{L}(\text{TTA})_4(\text{OAc})_2$ (**3**) at 77K.

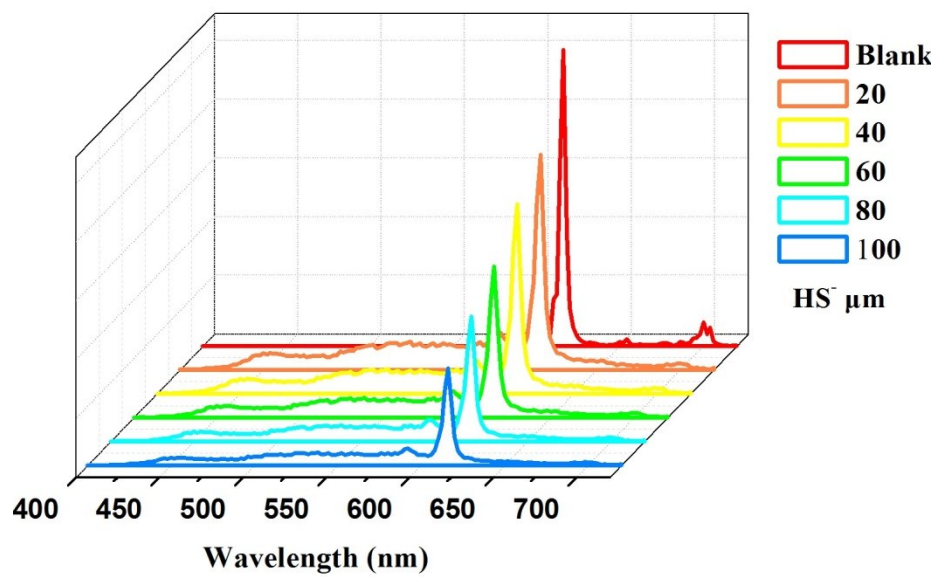


(a)

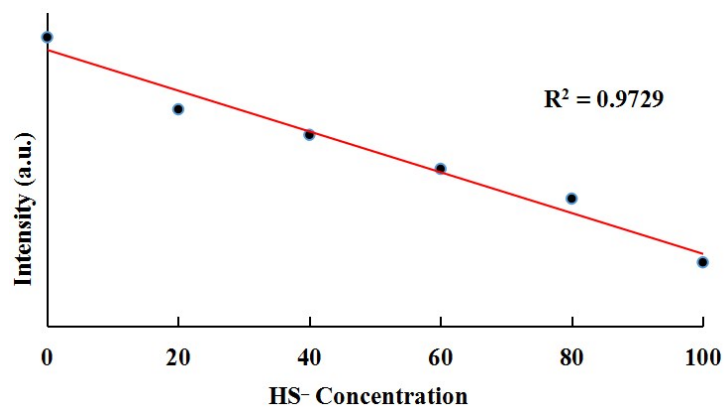


(b)

Fig.S9 (a) Emission spectra of doped complex $\text{Eu}_{0.2}\text{Gd}_{0.8}\text{TTA}$ upon incremental addition of acetic acid; (b) The calibration curve with the addition of acetic acid.

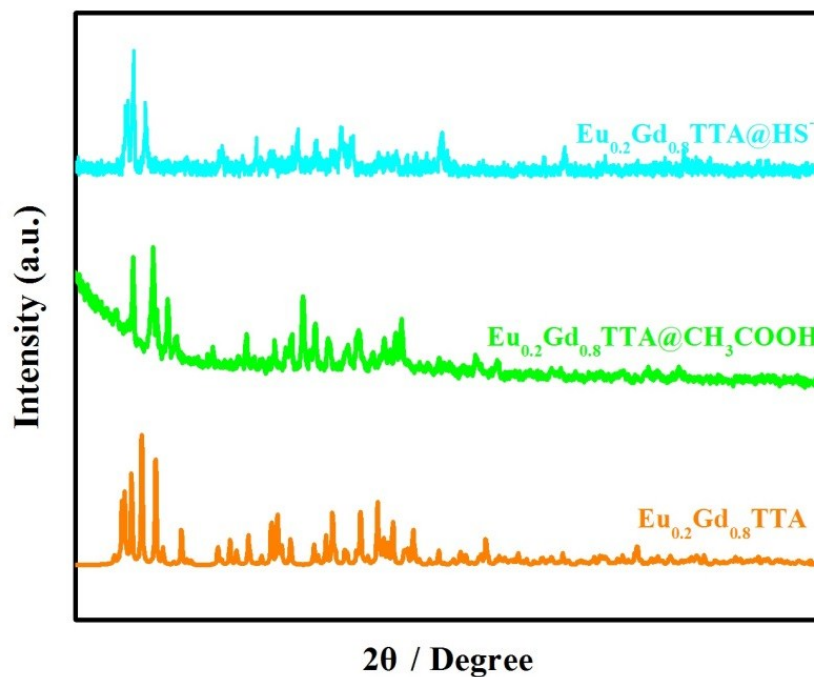


(a)

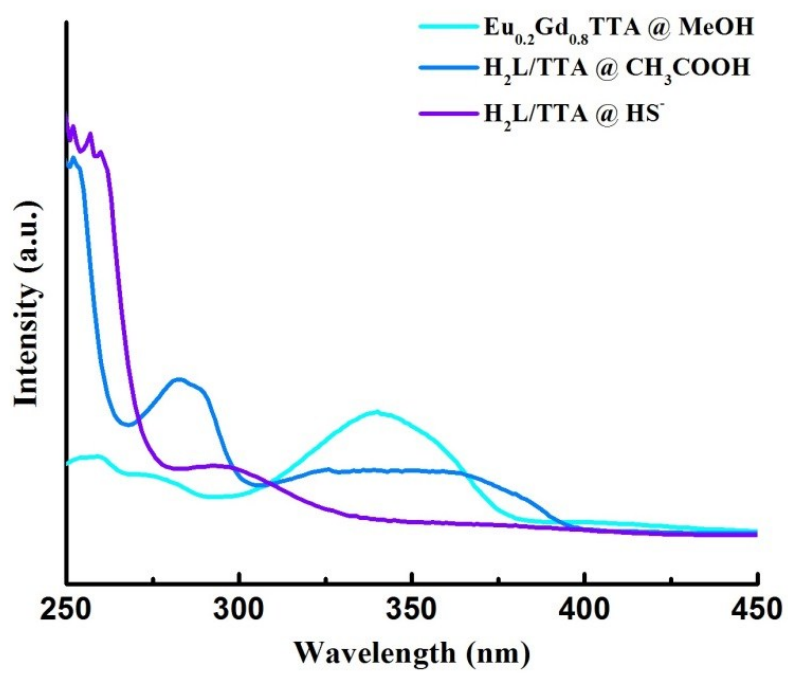


(b)

Fig.S10 (a) Emission spectra of complex $\text{Eu}_{0.2}\text{Gd}_{0.8}\text{TTA}$ with increasing concentration of HS^- ; (b) The calibration curve with increasing concentration of HS^- .



(a)



(b)

Fig.S11 (a) PXRD patterns for $\text{Eu}_{0.2}\text{Gd}_{0.8}\text{TTA}@CH_3COOH$ and HS^- ; (b) UV-vis absorption spectra of $\text{Eu}_{0.2}\text{Gd}_{0.8}\text{TTA}@MeOH$, $\text{H}_2\text{L}/\text{DBM}@CH_3COOH$ and HS^- .

Table S1 Elemental analysis of lanthanide ions by ICP for doped complexes $\text{Ln}_x\text{Gd}_{1-x}\text{TTA}$

Complex	$\text{Eu}_{0.2}\text{Gd}_{0.8}\text{TTA}$		$\text{Sm}_{0.2}\text{Gd}_{0.8}\text{TTA}$		$\text{Yb}_{0.05}\text{Gd}_{0.95}\text{TTA}$	
	Sm	Gd	Eu	Gd	Yb	Gd
Wt % (Found)	20.0	80.0	20.0	80.0	5.0	95.0
Mol%	19.2	80.8	18.9	81.1	4.4	95.6

Table S2 $[(\text{Ln}_x\text{Gd}_{1-x})_2\text{L}(\text{TTA})_4(\text{OAc})_2]_n$ – luminescence intensity ratio, lifetime and quantum yield of Ln^{3+} ions in corresponding doped materials.

Ln^{3+}	Sm^{3+} (1)	Eu^{3+} (2)	Yb^{3+} (4)
I/I_0	3.68	3.43	3.8
τ_0 (μs)	3.04 / 10.24	631.60	2.50 / 8.90
τ (μs)	37.43	717.15	18.95
φ_0 (%)	1.1	53.9	—
φ (%)	6.8	76.2	—

I_0 , τ_0 , φ_0 : $\text{Ln}_2\text{L}_2(\text{DBM})_4(\text{OAc})_2$; I , τ , φ : doped materials – $\text{Eu}_{0.2}\text{Gd}_{0.8}\text{TTA}$, $\text{Sm}_{0.2}\text{Gd}_{0.8}\text{TTA}$ and $\text{Yb}_{0.05}\text{Gd}_{0.95}\text{TTA}$

Table S3 The triplet energy levels of $\text{H}_2\text{L}/\text{TTA}$ and the energy gaps $\Delta E(\text{T}_1-\text{Ln}^{3+})$

	T_1	Eu^{3+}	Sm^{3+}	Yb^{3+}
Energy level (cm^{-1})	20161	17500	17924	10000
$\Delta E(\text{T}_1-\text{Ln}^{3+})$	—	2661	2237	10161